International Journal of Thermophysics, Vol. 22, No. 2, 2001

Optical Properties of Polyimide Films in the Infrared[1]

P. A. Kawka[2] and R. O. Buckius[2, 3]

The objective of this study is to determine the infrared optical constants of polyimide films in the spectral range between 2000 and 7000 cm^{-1} using a five-oscillator Lorentz model. Model parameters are presented, in addition to the derived values of the complex refractive index and dielectric constant. The parameters were obtained using electromagnetic theory for thin films to model reflectivity data from two film samples with different thicknesses (5.17 and 12.4 μm) on gold substrates examined at two incident angles. Measurements were taken using a polarizable reflectometer device in a Fourier transform infrared (FTIR) spectrometer. The real part of the refractive index, n, is shown to be about 1.67, while the imaginary part, k, is less than 0.01 over the spectral range examined. Results are consistent with findings of other experimentalists, and new data presented here show that polarization effects on thin film layers are predictable from the proposed model.

KEY WORDS: Fourier transform infrared (FTIR) spectrometer; Lorentz model; optical constants; polarization; polyimide films; radiative properties; reflectivity; refractive index.

1. INTRODUCTION

Thin film surfaces are common in engineering applications, affecting thermal transfer and optical phenomena in a wide range of scenarios, from oxide layers that form over most metals to manufacturing processes in microsystems. In the rapidly growing fields of integrated circuits (ICs) and microelectromechanical systems (MEMS), thin films play an important role in creating stress buffers, acting as dielectric materials, serving as optical

[1] Invited paper presented at the Fourteenth Symposium on Thermophysical Properties, June 25–30, 2000, Boulder, Colorado, U.S.A.

[2] Department of Mechanical and Industrial Engineering, University of Illinois at Urbana–Champaign, Urbana, Illinois 61801, U.S.A.

[3] To whom correspondence should be addressed. E-mail: buckius@uiuc.edu

0195-928X/01/0300-0517$19.50/0

waveguides, protecting and coating junctions, and forming structures [1–4]. Polyimide is one of the important materials used to create these coatings. Liquid polyimide precursors can be easily applied to a variety of substrates, manipulated using photoresists, etching techniques, and photolithography, and cured to provide a solvent resistant film structure useful for a variety of applications.

Because of its unique optical, electrical, and mechanical properties, several researchers have characterized polyimide for use in several applications. Some researchers have characterized polyimide properties for applications in liquid crystal displays (LCDs). The planar orientation of the long-chain polymers in spun polyimide films results in a small degree of negative birefringence. This property has been investigated by Li et al. [5] in the visible range to extend the viewing angles of twisted nematic LCDs. The application of negative birefringent polyimide compensates for the positive birefringence inherent in the liquid crystal. Other studies of polyimide for LCD application focus on the effect of film rubbing to orient the polyimide molecules, which in turn allows alignment of the liquid crystal molecules. Sakamoto et al. [6] and Lavers [7] have studied polyimide films using IR spectroscopy and attenuated total reflection (ATR) spectroscopy, respectively, to characterize the influence of film rubbing on the optical properties, molecular alignment, and surface roughness.

Optical properties of polymides have also been examined in the soft X-ray region from transmission measurements with Kramers–Kronig analysis and multiple-angle reflection measurements [8]. The motivation in this study was to characterize carefully errors in the optical property determination processes, compare two methods for finding optical constants, and provide useful X-ray optical properties for polyimide applicable to X-ray lithography.

Finally, optical property characterization of polyimide in the infrared between 500 and 6000 cm^{-1} has been performed by Zhang et al. [9] using unpolarized FTIR transmission measurements of films of varying thicknesses to facilitate design in filters and optoelectronic applications. Minimization of the RMS error and Lorentz modeling were both used to determine optical constants.

In this work, Fourier transform infrared (FTIR) spectroscopy is used to measure the bidirectional reflectivity (ρ'') of polyimide films on gold substrates in the infrared. The optical constants of cured polyimide are determined in the infrared region between 2000 and 7000 cm^{-1} (5 and 1.4 μm) using a Lorentz model to characterize the absorption bands. The effect of polarizing the incident and reflected radiation is examined to determine if the generally planar orientation of the molecules in the spun films affects the properties significantly. The model parameters that minimize

the RMS error between the experimental reflectivity measurements and the computed theoretical reflectivity from optical constants are reported.

2. EXPERIMENTS

2.1. Surface Fabrication

To determine the optical property characteristics of PI2723, two thin film test samples were fabricated in clean-room facilities at the University of Illinois Microelectronics Lab. Uncoated, unprotected 2.54-cm circular gold mirrors were obtained from Melles Griot (Part No. 02MFG015045) and served as substrates for the thin film samples. To prepare the samples, each mirror substrate was first cleaned using acetone, followed by isopropyl alcohol, followed by deionized water. Any remaining water was blown from the surface using filtered air, and the sample was placed briefly on a 110°C hot plate to complete drying. On each substrate, a small piece of tape was placed on the edge to serve as a mask to remove a small portion of subsequent layers of polyimide and allow easy measurement of the film thickness.

Each substrate was placed on a centripetal spinner set to run for 45 s at 2000 rpm. Five drops of PI2723 were then placed in the center of the sample using an eye dropper before the spinner was started. Soft curing of the samples on a hot plate followed the spinning procedure and lasted 4 min at 75°C. The above steps were repeated to add a second coating of film to one of the samples to create a thicker film layer. At this point, the pieces of masking tape were removed from the samples and the photosensitive PI samples were UV exposed at an intensity of about 2 to 3 $mW \cdot cm^{-3}$ to provide a 200 $mJ \cdot cm^{-3}$ dosage. The procedure presented closely follows the directions provided by HD Microsystems [10] for the usage of PI2723.

The final step in the sample preparation was an approximately 7-h vacuum annealing process to hard-cure the samples to a repeatable condition. First, the samples were placed in an open-air environment on a 60°C hot plate that ramps up to 150°C over 45 min. At 150°C, the samples were baked for 30 min before the hot plate was ramped up to 300°C over 75 min. At 300°C, a glass dome was placed over the sample and a roughing pump was used to bring the pressure down to about 5×10^{-4} Pa. A very low-flow N_2 bleed was initiated to prevent roughing pump oil from diffusing into the chamber. After baking for 30 min at 300°C in the vacuum, the hot plate was ramped up to 450°C over 75 min. The samples were baked for 45 min at 450°C. Finally, the samples were allowed to cool to 60°C for about 2 h in a vacuum environment before being removed.

After vacuum annealing, a Tencor Instruments Alpha Step 200 physical profilometer was used to measure film thicknesses for each sample by

measuring the height of the step created by the masking process. The single layer sample was found to have a film height (h) of $5.17 \pm 0.20\ \mu$m, and the double-coated sample had a film thickness of $12.5 \pm 0.8\ \mu$m. The samples were then stored in a desiccated environment to minimize water absorption by the polyimide films.

2.2. Reflection Measurements

To determine the optical constants of the PI2723 material, a Nicolet Magna-IR 750 Fourier transform infrared (FTIR) spectrometer was used with a reflectometer apparatus to measure the in-plane reflectivity of the samples. The reflectometer system is based on a modified Seagull variable-angle reflectivity accessory from Harrick Scientific Corporation and allows the collection of in-plane bidirectional reflectivity data. Polarizers are fixed on the inlet and outlet ports to allow selection of polarized radiation parallel or perpendicular to the plane of incidence. Using a liquid nitrogen-cooled mercury cadmium telluride (MCT) quantum detector and an air-cooled Ever-Glo source operating at 1500 K, the FTIR spectrometer is capable of measuring the reflected energy from the surface as a function of wave number ranging from about 650 to 7000 cm^{-1} (15.38 to 1.43 μm). For all measurements reported in this research, 256 spectral scans were averaged, with a resolution of 32 cm^{-1}. The incident and reflected solid angles for the system are known to be approximately 3° [11].

An uncoated gold mirror identical to the film sample substrates was used as reference material and was assumed to have known spectral dependent optical properties, n and k, given by Brewster [12]. To be able to use the gold properties at discrete values over a large range of wave numbers, the data were fit using power law relationships that represented the n and k data points with a maximum error of less than 3.2% and an average error of less than 1.3%.

Reflection data of each surface of PI 2723 thin film were taken for incident angles of 30 and 45° and for ss (entry and exit perpendicular to plane of incidence) and pp (entry and exit parallel to plane of incidence) polarizations. Cross-polarization (sp and ps) was also examined and shown to contain a negligible amount of energy that was below the measurement threshold of the FTIR system. Using a relative method, the bidirectional spectral reflectivities of samples can be determined using the following equation [11]:

$$\rho''_{\lambda}(\Omega_{\mathrm{i}}, \Omega_{\mathrm{r}}) = \rho''_{\lambda,\,\mathrm{ref}}(\Omega_{\mathrm{i}}, \Omega_{\mathrm{r}}) \frac{V_{\mathrm{m}}}{V_{\mathrm{ref}}} \tag{1}$$

where ρ''_λ is the bidirectional spectral reflectivity, and V_m and V_{ref} are the experimentally measured voltages for the sample and reference. All measurements were performed for the same incident and reflected solid angles.

3. ANALYSIS

For a general surface, bidirectional reflectivity is the fundamental measure of its reflection characteristics. It is defined as the ratio of π times the reflected intensity over the incident partial flux and is, in general, a function of the wavelength and the incident and reflected angles. It can be expressed as

$$\rho''_\lambda(\Omega_i; \Omega_r) = \frac{\pi I_{\lambda_r}(\Omega_r)}{I_{\lambda_i}(\Omega_i) \cos\theta_i \, d\Omega_i} \tag{2}$$

where I is the intensity, Ω is the solid angle, θ is a polar angle, λ is a wavelength, and the subscripts i and r denote incident and reflected intensity, respectively [12].

In this study, both the film-coated substrates and the reference mirror are assumed to produce specular reflections in the infrared region. For ideal specular reflection, bidirectional reflectivity ρ'' can be related to hemispherical reflectivity using

$$\rho''_\lambda = \pi\rho'_\lambda \frac{\delta(\theta_r - \theta)\,\delta(\phi - \phi_r + \pi)}{\cos\theta \sin\theta} \tag{3}$$

where δ is the Dirac delta function and ϕ is the azimuthal angle. In these experiments, assuming that the incident energy is reflected nearly specularly and all of the energy is captured in the system's solid angle about the reflected angle, it is possible to combine Eqs. (1) and (2) to allow direct computation of the hemispherical reflectivity using

$$\rho'_\lambda(\Omega_i, \Omega_r) = \rho'_{\lambda,\,ref}(\Omega_i, \Omega_r) \frac{V_m}{V_{ref}} \tag{4}$$

The assumption of nearly specular reflection allows comparison with electromagnetic theory results for layered media. Layer reflectivity [12, 13] is found using

$$\rho'_{film} = \left| \frac{r_{12} + r_{23} e^{-i2\tilde{\beta}}}{1 + r_{12} r_{23} e^{-i2\tilde{\beta}}} \right|^2 \tag{5}$$

where

$$\tilde{\beta} = \frac{2\pi \tilde{n}_2 h \cos \tilde{\theta}_2}{\lambda_0} \tag{6}$$

and the Fresnel coefficients or complex amplitude ratios are given by

$$r_{\mathrm{ab}\parallel} = \frac{\tilde{n}_\mathrm{b} \cos \tilde{\theta}_\mathrm{a} - \tilde{n}_\mathrm{a} \cos \tilde{\theta}_\mathrm{b}}{\tilde{n}_\mathrm{b} \cos \tilde{\theta}_\mathrm{a} + \tilde{n}_\mathrm{a} \cos \tilde{\theta}_\mathrm{b}} \tag{7}$$

$$r_{\mathrm{ab}\perp} = \frac{\tilde{n}_\mathrm{a} \cos \tilde{\theta}_\mathrm{a} - \tilde{n}_\mathrm{b} \cos \tilde{\theta}_\mathrm{b}}{\tilde{n}_\mathrm{a} \cos \tilde{\theta}_\mathrm{a} + \tilde{n}_\mathrm{b} \cos \tilde{\theta}_\mathrm{b}} \tag{8}$$

In Eqs. (5) and (6), r is the interface reflectivity and the subscripts 1, 2, and 3 represent the different media, where 1 corresponds to air having a purely real refractive index ($n = 1.0$), 2 is the polyimide film, and 3 is the gold substrate. The subscripts a and b represent different choices of material numbers (1, 2, or 3) to describe a reflection coefficient when a wave is incident from medium a to medium b. The symbol $\tilde{n}$ is the complex refractive index, given as $n - ik$, and $\tilde{\theta}$ is a complex representation of the angle of propagation in the media. For a medium with no absorption ($k = 0$), θ is the angle of propagation in the medium measured from the normal. The propagation angles in the different media are related by Snell's law as

$$\tilde{n}_\mathrm{a} \sin \tilde{\theta}_\mathrm{a} = \tilde{n}_\mathrm{b} \sin \tilde{\theta}_\mathrm{b} \tag{9}$$

In addition, the complex refractive index, $\tilde{n}$, can be represented equivalently by the complex dielectric constant given by

$$\tilde{\varepsilon}_\mathrm{r} = \varepsilon_\mathrm{r}' - i\varepsilon_\mathrm{r}'' = \tilde{n}^2 \tag{10}$$

where ε_r' and ε_r'' are the real and imaginary parts of the relative permitivitty.

In general, the optical constants of a material vary spectrally and often can be modeled using a damped oscillator or Lorentz model. Under the assumptions that a material is composed of charged particles held in place by isotropic elastic forces, and affected by isotropic linear damping forces, it can be shown that for a single oscillator,

$$\tilde{\varepsilon}_\mathrm{r} = \tilde{n}^2 = 1 + \frac{\omega_\mathrm{p}^2}{\omega_0^2 - \omega^2 + i\gamma\omega} \tag{11}$$

where ω_p is the plasma frequency, ω_0 is the oscillator frequency, and γ is the relaxation frequency [12, 14]. A multiple oscillator model of this type

is used to characterize the spectral optical constants of polyimide in the infrared. The oscillator model in Eqs. (10) and (11) provides the dielectric constants given by

$$\varepsilon'_r = n^2 - k^2 = n_e^2 + \sum_{j=1}^{5} \frac{\omega_{pj}^2(\omega_{0j}^2 - \omega^2)}{(\omega_{0j}^2 - \omega^2)^2 + \gamma_j^2\omega^2} \tag{12}$$

$$\varepsilon''_r = 2nk = \sum_{j=1}^{5} \frac{\omega_{pj}^2\gamma_j\omega}{(\omega_{0j}^2 - \omega^2)^2 + \gamma_j^2\omega^2} \tag{13}$$

and the indices of refraction given as

$$n = \left[\frac{\varepsilon'_r + \sqrt{\varepsilon'^2_r + \varepsilon''^2_r}}{2}\right]^{1/2} \tag{14}$$

$$k = \left[\frac{-\varepsilon'_r + \sqrt{\varepsilon'^2_r + \varepsilon''^2_r}}{2}\right]^{1/2} \tag{15}$$

The measured reflectivity properties are used to determine the refractive index using the electromagnetic theory presented in Eqs. (5)–(9). The film reflectivity prediction from these equations is for a single specular angle of incidence and reflection. Therefore, results were averaged over a solid angle of 3° to correspond to the conditions of the experimental data as closely as possible. Spectral averaging over 32 cm^{-1} was not performed because the reflectivity does not change very significantly within each 32 cm^{-1} interval over the spectral region from 2000 to 7000 cm^{-1}. Spectral averaging would not have a significant effect on the accuracy of the results (maximum single data point change of $<2\%$).

The eight sets of data obtained from the three independent parameters of incident angle (30 or 45°), film thickness (5.17 or 12.5 μm), and polarization (pp, ss) were reduced to four sets of data by averaging the pp and ss polarizations. From the four sets of reflectivity data, it was observed that no significant absorption bands appeared between 4000 and 7000 cm^{-1}. Therefore, this region was used to assess and evaluate the values of the PI film thicknesses (h_1, h_2) and the optical constant n_e (assuming $k = 0$) that predict the layer reflectivities that best fit the measured data. The subscript e represents an equivalent value that accounts for contributions to the refractive index from oscillators at frequencies lower than the region of interest.

The film thicknesses h_1 and h_2 were allowed to vary only within the range of $\pm 10\%$ of the experimentally measured values, to allow for the possibility of some error in measurements and the variation of thickness with position. The best fit of the data was obtained by varying the four

Table I. Parameters for the Five-Oscillator Model

	h_1 (μm) = 5.17	h_2 (μm) = 12.4		$n_e = 1.68$	
	Oscillator 1	Oscillator 2	Oscillator 3	Oscillator 4	Oscillator 5
ω_p (rad · s^{-1})	0.284	0.0611	0.0344	0.0541	0.0341
ω_0 (rad · s^{-1})	1.079	1.834	1.929	2.188	2.281
γ (rad · s^{-1})	0.0123	0.0799	0.0456	0.124	0.0432
η (cm^{-1})	1717	2919	3070	3482	3630

parameters until the spectrally averaged RMS difference between the theoretical prediction and the experimental values was minimized. The values of h_1 and h_2 are 5.17 and 12.4 μm, respectively, as noted in Table I.

With the film thickness and high-wave number (high-frequency) optical constants evaluated, the spectral region between about 2000 and 4000 cm^{-1} was then examined to determine the spectral variation of n and k due to absorption bands in the film. To treat the absorption bands between 2000 and 4000 cm^{-1}, a five-oscillator Lorentz model was applied to the spectral region in a treatment similar to that performed by Zhang et al. [9] and Sakamoto [15]. The locations of the oscillators (ω_{0i}) were determined through a combination of data inspection, reported values in the literature [16], and error minimization. At each oscillator location, the two remaining oscillator parameters, ω_p and γ, controlling the oscillator strength and width, respectively, were varied to minimize the error in the prediction and are given in Table I. The theoretical reflectivity curve is obtained using Eqs. (5)–(9), using the fitted optical properties from the oscillator model.

4. RESULTS AND DISCUSSION

The experimental reflectivity data for the four cases examined (30 and 45° incidence and 5.17- and 12.4-μm layer thicknesses) are compared to the reflectivity computed from the model results in Figs. 1 to 4. Each figure shows the model prediction and experimental results for ss, pp, and averaged polarizations. The maximum and average errors between the reflectivity calculated from the model and the experimental results for each case of averaged polarization are computed and given in Table II.

The error statistics from Table II indicate that the five-oscillator model well represents the experimental results on a spectrally averaged and polarization averaged basis from 2000 to 7000 cm^{-1}. The spectrally averaged absolute error is less than 4% for all four cases, and the spectrally

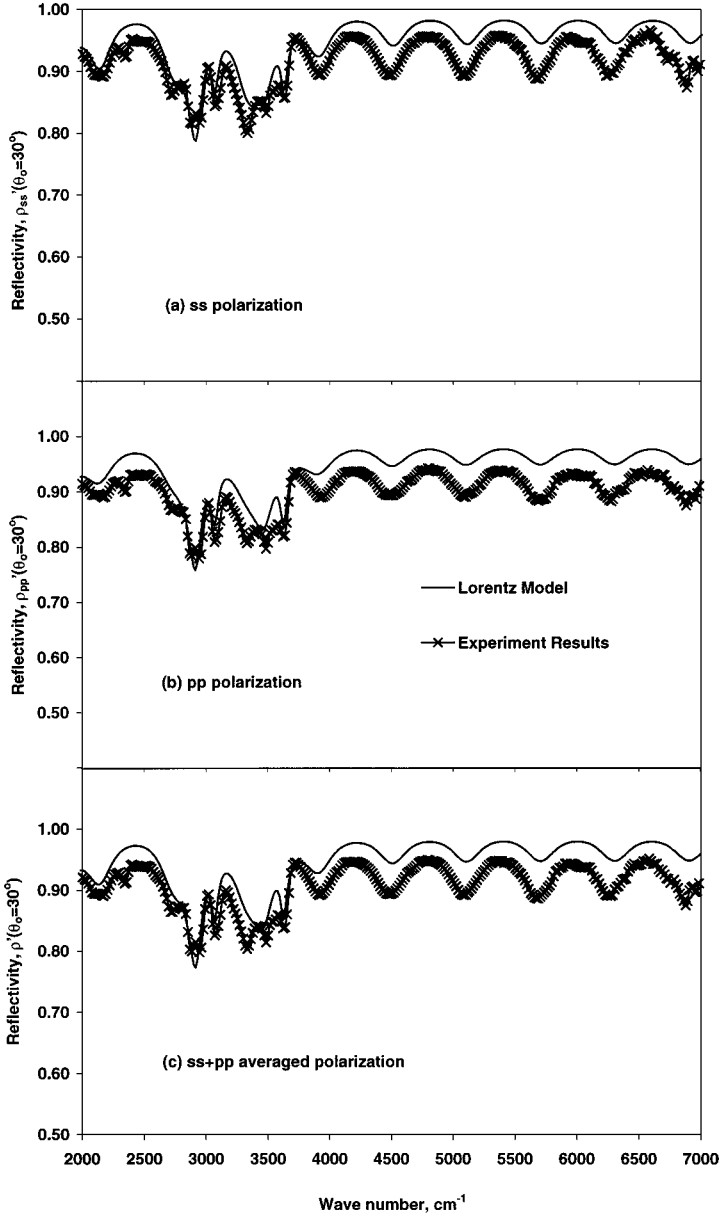

Fig. 1. (a)–(c) Comparison of experimental and predicted layer reflectivity for PI2723 film with a 5.17-μm thickness at 30° incidence.

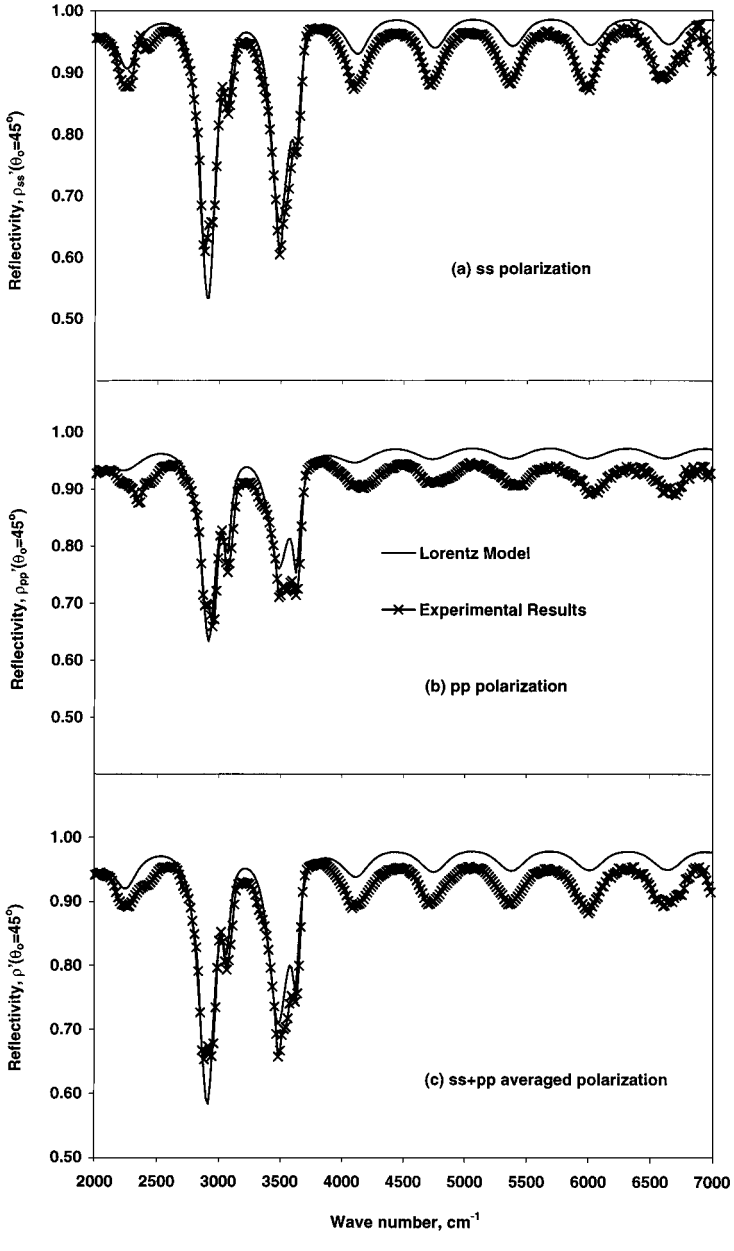

Fig. 2. (a)–(c) Comparison of experimental and predicted layer reflectivity for PI2723 film with a 5.17-μm thickness at 45° incidence.

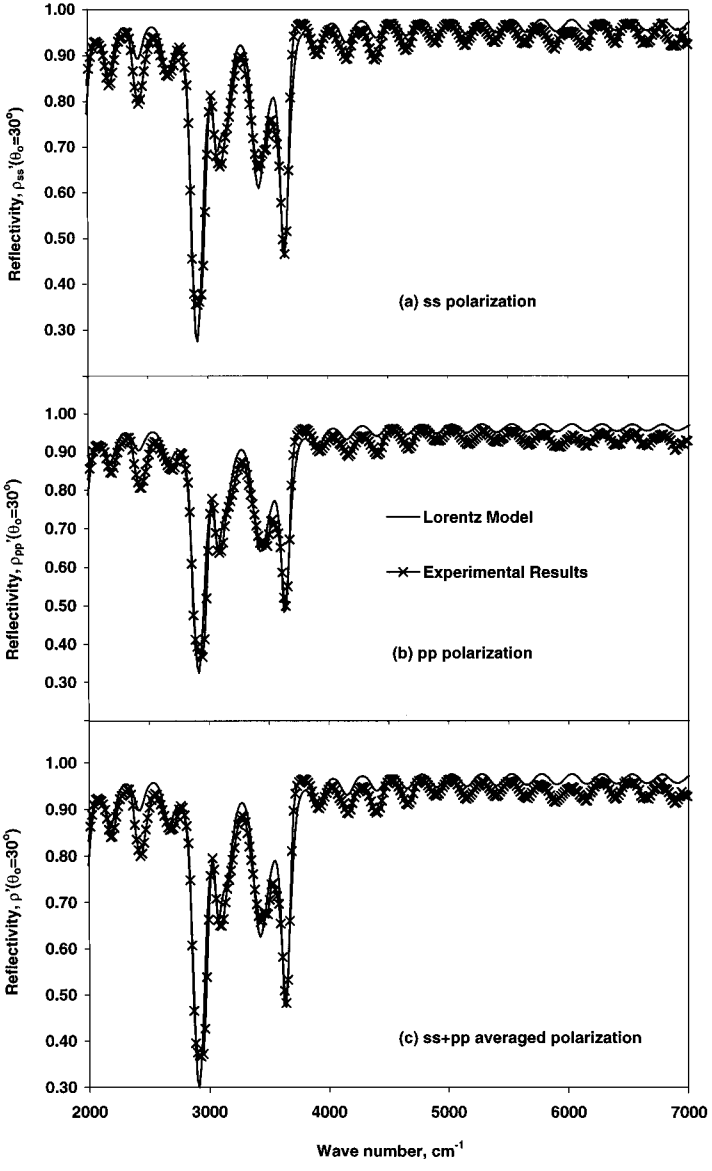

Fig. 3. (a)–(c) Comparison of experimental and predicted layer reflectivity for PI2723 film with a 12.4-μm thickness at 30° incidence.

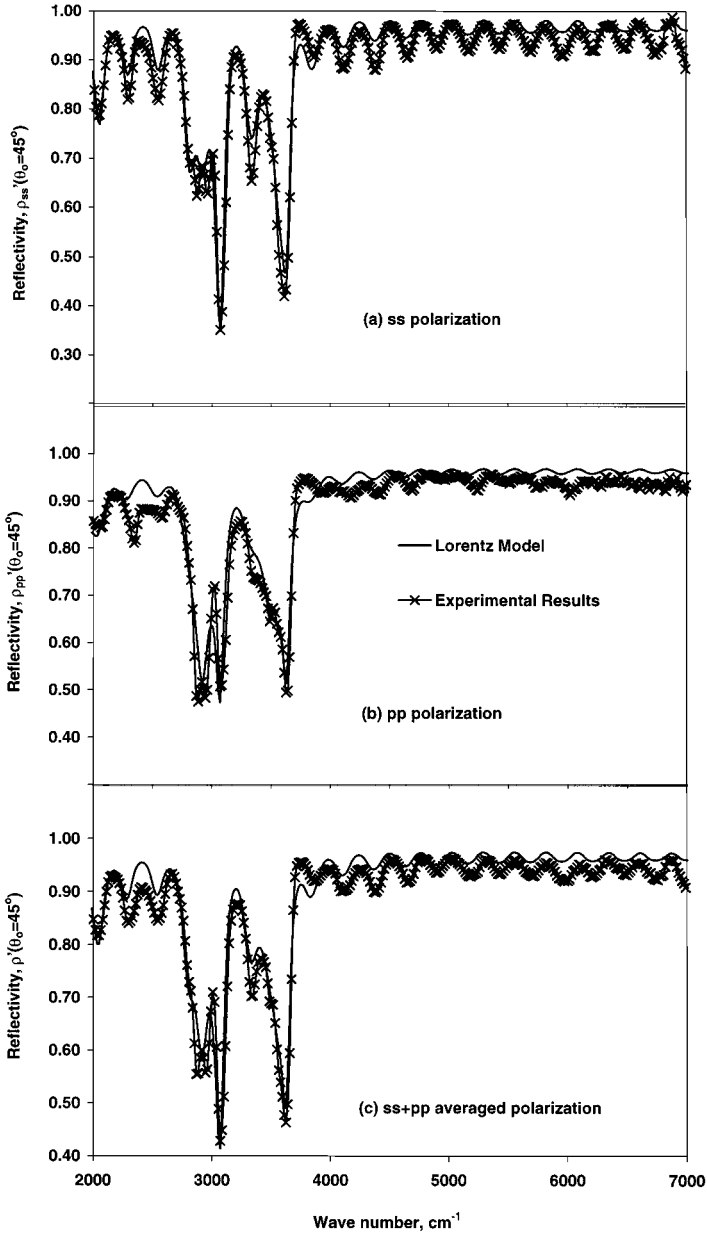

Fig. 4. (a)–(c) Comparison of experimental and predicted layer reflectivity for PI2723 film with a 12.4-μm thickness at 45° incidence.

Table II. Maximum and Spectrally Averaged Error Between Model Prediction and Experimental Reflectivity for Averaged Polarizations

Sample	Maximum absolute error (%)	Spectrally averaged absolute error (%)	Spectrally averaged RMS error
30°, 5.17 μm	8.52	3.95	0.0421
30°, 12.4 μm	28.7	3.20	0.0400
45°, 5.17 μm	13.4	3.49	0.0397
45°, 12.4 μm	19.4	3.24	0.0441

averaged RMS error is less than 0.045. The single data point maximum error is 29% and occurs in the case with 30° incidence on a 12.4-μm film. This error occurs at a wave number of 2962 cm^{-1} that is in the vicinity of an absorption band and is the general spectral region of the largest single point errors for both 45° incident cases as well. With results obtained from the five-oscillator model, the experimental data are well represented in both magnitude and trend. Any large changes in reflectivity due to absorption bands and the superimposed ripples from interference effects are qualitatively captured by the theoretical curve fit, even though it is not able to predict all the fine details. Some overprediction and underprediction of the reflectivity do occur at the locations corresponding to the greatest property changes. In addition, in the spectral region from about 4000 to 7000 cm^{-1}, where no absorption bands are observed, the model has a relatively constant level of error. The model predicts a reflection that is about 4.5% too high for the 5.17-μm samples and is about 2.5% too high for the 12.4-μm samples. This systematic offset of difference between the experiments and the model is most likely due to measurement errors in the FTIR system and assumptions made in the analysis. It is likely that roughness in the film surface and minor shifts in the focal plane from using surfaces with varying film thickness cause the assumption of a flat specular film to be less accurate. Some energy is therefore not captured in the reflected solid angle, resulting in experimental values lower than the predicted values. The increasing effect of film roughness and decreasing signal can be observed in Fig. 4b, showing pp polarized reflection of the thicker and rougher two-layer sample. At higher wave numbers (shorter wavelengths), the interference becomes less distinguishable and deviates from its smooth periodicity.

The spectral variation of the optical properties based on the model is presented in Fig. 5 as n and k and in Fig. 6 as ε_r' and ε_r''. From the variations in n or ε' and the peaks in k or ε'', the contributions of four of the five oscillators are clearly distinguished. The fifth oscillator exists at a location just below 2000 cm^{-1} and is responsible for the initial increase in n

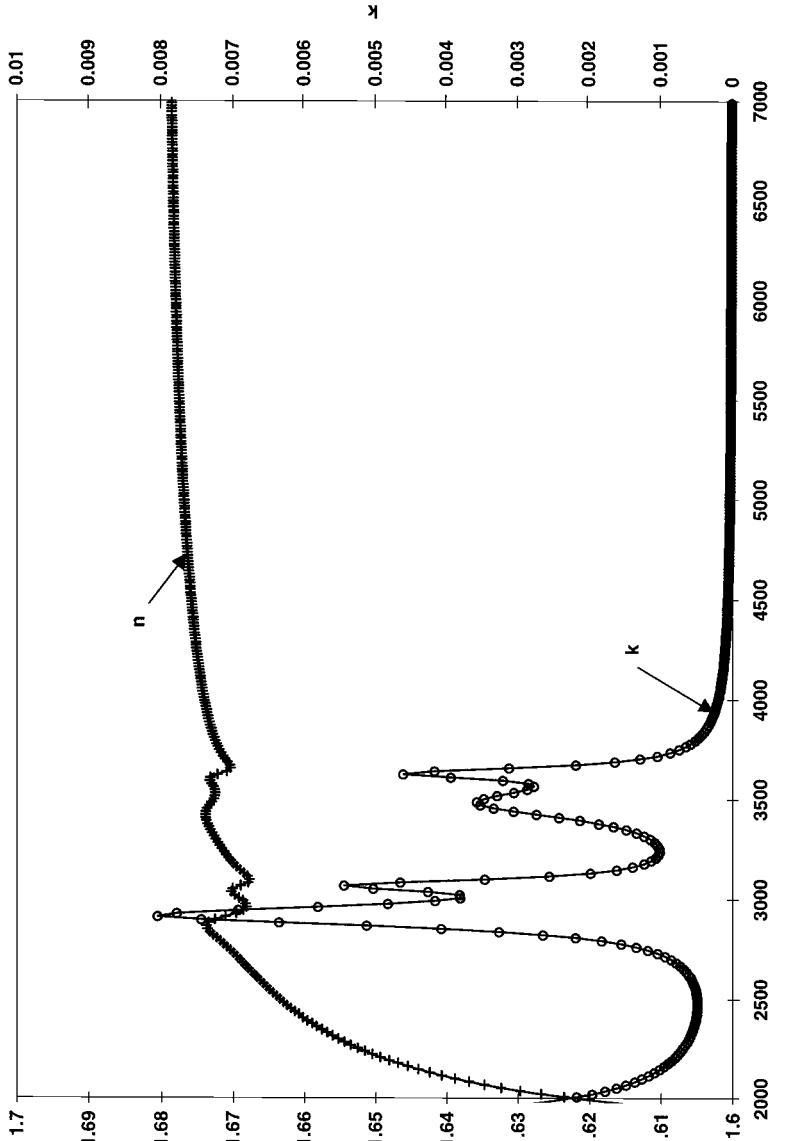

Fig. 5. Optical constants n and k versus wave number for PI2723 from the five-oscillator model.

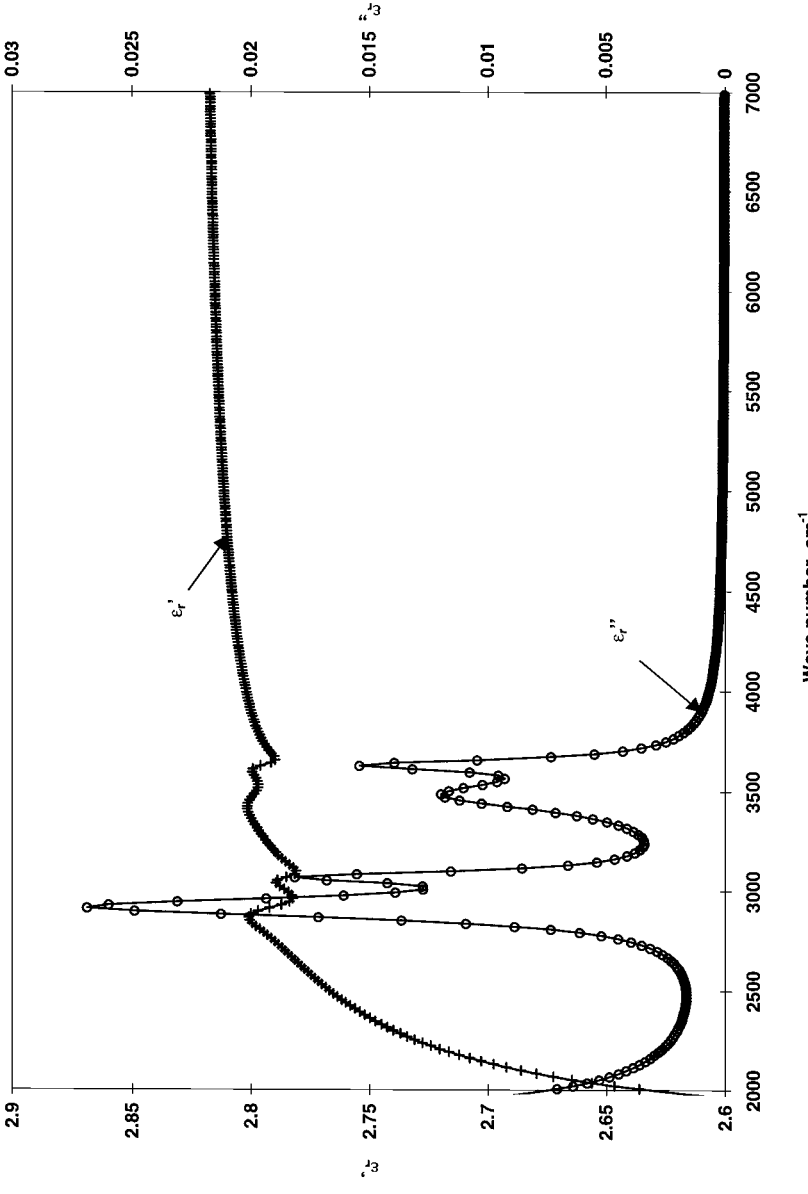

Fig. 6. Dielectric constants ε_r' and ε_r'' versus wave number for PI2723 from the five-oscillator model.

and ε' and the initial decrease in k and ε''. The real parts of the refractive index and dielectric constant, n and ε', do not vary significantly in the spectral region from 2000 to 7000 cm^{-1}. Both begin at a minimum value, increase rapidly, and level off to a steady value corresponding to $n_e = 1.68$ that is less than 7% higher than the initial value. Small variations in n and ε' occur, consisting of an increase followed by a decrease followed by an increase at the locations of the oscillators. For the complex part of the refractive index and dielectric constant, k and ε'', local peaks occur at the locations of the oscillators and the maximum value occurs at 2919 cm^{-1}, where the strongest oscillator between 2000 and 7000 cm^{-1} exists. At high wave numbers, the complex part drops to a very small value, approaching 0 for increasing wave numbers.

Overall, the results presented in this study are consistent with the findings of other researchers. The values of n varying from 1.64 to 1.68 over the spectral range from 2000 to 7000 cm^{-1} are between the value of 1.59 obtained by Saito et al. [17] and the values of 1.73 to 1.75 in the spectral region between 2500 and 6000 cm^{-1} obtained by Zhang et al. [9]. The imaginary part of the refractive index was less than 0.01 over the entire region examined and was less than 0.001 between 4000 and 7000 cm^{-1}. Peaks occurred at the location of the absorption bands as indicated in Fig. 5.

Even though the Lorentz model was developed using the averaged polarization effects, the values of n and k that it provides also accurately predict polarized reflection distributions. The reflectivity values for the polarized cases are again obtained using the electromagnetic theory for thin films [Eqs. (5)–(9)]. Even though electromagnetic film theory assumes homogeneous and isotropic optical properties within the film, the results are correct to within the same error levels obtained for the averaged polarization case. This result indicates that even though the polyimide polymer material has long-chain molecules and has been shown to demonstrate anisotropic optical properties in studies by Hardaker et al. [3], Sakamoto et al. [6], Lavers et al. [7], and Goeschel et al. [18], these effects in spin-coated, planar layers are small compared with the spectral variation of the optical properties.

Overall, possible errors that affect the accuracy and applicability of the model presented are numerous. First, the properties of the gold-coated substrate were not directly measured but were obtained from the literature. Differences between the actual substrate properties and the tabulated properties used are unknown but should not have a large affect on the results because model parameters were derived based on reflectivity calculations. Because the optical properties of gold in the infrared lead to a very high and a relatively constant reflectivity, error from the characterization of the gold should not be very significant. Uncertainties also exist

in the preparation and characterization of the polyimide films. Any roughness in the film layer causes some energy to be reflected off-specular that may not be collected in the solid angles of the reflectometer. This nonideality would result in experimental reflectivities lower than those being predicted by theory for an equivalent set of parameters. In addition, polyimides have a complex chemical nature, and although measures were taken to cure the polyimide fully at a high temperature in a vacuum oven to produce repeatable conditions, processing, storage, and aging of a film should affect its properties. Finally, uncertainties introduced simply from the use of the FTIR system described have been determined to be less than 10% [11].

5. CONCLUSIONS

This study provides parameters for a five-oscillator Lorentz model of the thin film optical properties of PI2723 in the infrared from 2000 to 7000 cm^{-1} when it is prepared using the standard procedures. Experimental reflectivity measurements of a polyimide film over gold were taken using FTIR spectroscopy. Model parameters were computed through minimization of the average spectral rms error between the experimental results in four cases and the theoretical film reflectivity computed using Fresnel relations, electromagnetic theory, and the model parameters. The low values of average, rms, and maximum error indicate the accuracy of the model. Polarization effects on the optical properties of spin-coated films are shown to be less significant than spectral variations in the optical properties.

ACKNOWLEDGMENTS

This research was supported, in part, by the National Science Foundation (NSF CTS 95-31772) and utilized the University of Illinois Microelectronics Lab facilities for sample preparation. The polyimide used in this work was obtained from the BioMEMS group headed by Professor David J. Beebe.

REFERENCES

1. P. Y. Wong, B. D. Heilman, and I. N. Miaoulis, *Microscale Heat Transfer* **291**:27 (1994).
2. A. R. Abramson and C. L. Tien, *Microscale Therm. Eng.* **3**:229 (1999).
3. S. S. Hardaker, S. Moghazy, C. Y. Cha, and R. J. Samuels, *J. Polym. Sci. Pol. Phys.* **31**:1951 (1993).
4. K. R. Ha and J. L. West, *Mol. Cryst. Liq. Cryst.* **323**:129 (1998)
5. B. Li, T. He, and M. Ding, *Thin Solid Films* **320**:280 (1998).
6. K. Sakamoto, R. Arafune, and S. Ushioda, *Appl. Spectrosc.* **51**:541 (1997).

7. C. R. Lavers, *Thin Solid Films* **289**:133 (1996).
8. R. Wolf, H. G. Birken, and C. Kunz, *Appl. Opt.* **31**:7313 (1992).
9. Z. M. Zhang, G. Lefever-Burton, and F. R. Powell, *Int. J. Thermophys.* **19**:905 (1998).
10. HD Microsystems, *Pyralin® PI2720 Processing Guidelines* (1998), pp. 1–16.
11. J. N. Ford, K. Tang, and R. O. Buckius, *J. Heat Transfer* **117**:955 (1995).
12. M. Q. Brewster, *Thermal Radiative Transfer and Properties* (Wiley, New York, 1992), pp. 114–152, 504.
13. M. Born and E. Wolf, *Principles of Optics*, 6th ed. (Pergamon, Oxford, 1980), Chaps. 1, 13.
14. C. F. Bohren and D. R. Huffman, *Absorption and Scattering of Light by Small Particles* (Wiley, New York, 1983), Chap. 9.
15. K. Sakamoto, R. Arafune, S. Ushioda, Y. Suzuki, and S. Morokawa, *J. Appl. Phys.* **80**:431 (1996).
16. H. Ishida and M. T. Huang, *J. Polym. Sci. Pol. Phys.* **32**:2271 (1994).
17. M. Saito, T. Gojo, Y. Kato, and M. Miyagi, *Infrared Phys. Tecnhol.* **36**:1125 (1995).
18. U. Goeschel, H. Lee, D. Y. Yoon, R. L. Siemens, B. A. Smith, and W. Volksen, *Colloid Polym. Sci.* **272**:1388 (1994).